Available online at www.sciencedirect.com
ScienceDirect
Organic Electronics 8 (2007) 606–614
Organic Electronics
www.elsevier.com/locate/orgel

Energy level alignment and morphology of interfaces between molecular and polymeric organic semiconductors

F.J. Zhang [a,b], A. Vollmer [c], J. Zhang [b], Z. Xu [a], J.P. Rabe [b], N. Koch [b,*]

[a] *Key Laboratory of Luminescence and Optical Information, Ministry of Education, Institute of Optoelectronic Technology, Beijing Jiaotong University, Beijing 100044, China*
[b] *Institut für Physik, Humboldt-Universität zu Berlin, Newtonstr. 15, D-12489 Berlin, Germany*
[c] *Berliner Elektronenspeicherring-Gesellschaft für Synchrotronstrahlung m.b.H., Albert-Einstein-Str. 15, D-12489 Berlin, Germany*

Received 17 January 2007; received in revised form 1 April 2007; accepted 27 April 2007
Available online 23 May 2007

Abstract

Ultraviolet photoelectron spectroscopy (UPS) was used to determine the energy level alignment at organic–organic conductor–semiconductor and semiconductor–semiconductor hetero-interfaces that are relevant for organic optoelectronic devices. Such interfaces were formed by *in situ* vacuum sublimation of small molecular materials [C_{60} and pentacene (PEN)] and *ex situ* spin-coating of poly(3-hexylthiophene) (P3HT), all on the common substrate poly(3,4-ethylenedioxythiophene)/poly(styrenesulfonate) (PEDOT:PSS). We found that the deposition sequence had a significant impact on the interface energetics. The hole injection barrier (HIB) of C_{60} on PEDOT:PSS could be changed from 1.0 eV (moderate hole injection) to 1.7 eV (good electron injection) by introducing a layer of P3HT. The HIB of P3HT/PEDOT:PSS was increased by 0.35 eV due to an interfacial PEN layer. However, PEN deposited on PEDOT:PSS and P3HT/PEDOT:PSS exhibited the same value. These observations are explained by material-dependent dipoles at the interfaces towards PEDOT:PSS and substrate dependent inter-molecular conformation.

PACS: 73.20.−r; 73.61.Ph; 68.37.Ps

Keywords: Organic semiconductors; Interfaces; Photoelectron spectroscopy; Atomic force microscopy

1. Introduction

The physico-chemical properties of interfaces in organic optoelectronic devices, such as organic light emitting diodes (OLEDs), organic photovoltaic cells (OPVCs), and organic thin film transistors (OTFTs), largely determine device function and performance [1–5]. For instance, the importance of the energy level alignment at organic–metal interfaces has been pointed out in many studies [6–8]. However, comparably little is known about the energy level alignment at organic–organic hetero-interfaces [9–15], which is essential for further understanding and optimizing organic devices. Such hetero-interfaces are ubiquitous in modern devices, in order to facilitate efficient charge recombination (in OLEDs)

* Corresponding author. Tel.: +49 3020937819; fax: +49 3020937632.
E-mail address: norbert.koch@physik.hu-berlin.de (N. Koch).

1566-1199/$ - see front matter
doi:10.1016/j.orgel.2007.04.010

or charge separation (in OPVCs). Even fewer studies exist on interfaces formed between molecular and polymeric organic semiconductor interfaces [16], despite the potentially interesting structures resulting from that particular material combination. Here, we present studies on the energy level alignment at interfaces between two molecular materials (C_{60} and pentacene) and one polymeric organic semiconductor [poly(3-hexylthiophene)], with the conducting organic polymer mixture poly(3,4-ethylenedioxythiophene)/poly(styrenesulfonate) as common substrate. These prototypical organic materials are representative for the use in present OPVCs and OTFTs. Ultraviolet photoemission spectroscopy (UPS) was used to assess the relative positions of the highest occupied levels of the organic materials relative to the substrate Fermi-level, and the magnitude of interface dipoles. Furthermore, we investigated the influence of the deposition sequence of a polymer and a molecular material pair on the interface energetics, which has not been reported to date. Complementary investigations by atomic force microscopy (AFM) revealed that also the sample morphology was strongly influenced by the deposition sequence.

2. Experimental

Indium-tin-oxide (ITO) coated glass substrates (with a sheet resistivity 30 Ω/sq.) were cleaned by ultrasonication in acetone, ethanol and deionized water. An aqueous dispersion of poly(3,4-ethylenedioxythiophene):poly(styrenesulphonate) (Baytron P CH8000®, H.C. Starck GmbH & Co. KG) was spin-coated onto ITO/glass substrates and annealed at 200 °C for 5 min in ambient air. These conducting polymer/ITO stacks were used as substrates throughout this study. P3HT (Aldrich) was spin-coated (600 rounds per minute) *ex situ* from chloroform solution (0.2 mg/ml). Pentacene (Aldrich) and C_{60} (Aldrich) were evaporated from resistively heated pinhole sources in a preparation chamber directly attached to the analysis chamber of the experimental setup used for photoemission experiments (SurIcat at beamline PM4) at the synchrotron light source BESSY Gmbh (Berlin). The chemical structures of the used materials are shown in Fig. 1. The molecular film thickness was monitored with a quartz microbalance, and a typical evaporation rate of 0.2 nm/min was used. Photoemission spectra were collected with a hemispherical energy analyzer (Scienta SES 100) set to an energy resolution of 100 meV. The photon energy was 35 eV or 45 eV, as indicated in the respective spectra shown below. The secondary electron cutoff (for determination of sample work function and molecular ionization energy) was measured with −10.00 V sample bias. The positions of the low binding energy photoemission onsets and the secondary electron cutoffs were determined by the intersection of the tangents to peaks at the half-width position and the baseline.

The morphology of molecule-on-polymer and polymer-on-molecule heterostructures was investigated *ex situ* by atomic force microscopy (AFM), using a multimode nanoscope IV (Veeco) operated in tapping mode.

3. Result and discussion

3.1. C_{60} on PEDOT:PSS

First, C_{60} was deposited onto PEDOT:PSS/ITO in steps of increasing thickness. UPS spectra at each step were recorded as shown in Fig. 2a, with the Fermi-level (E_F) as binding energy (BE) reference. For 1 nm C_{60} on PEDOT:PSS, the emission from PEDOT:PSS was already strongly attenuated, and the characteristic photoemission of the valence levels of the organic material became apparent. The low BE onset of the highest occupied molecular orbital (HOMO) was found 1.1 eV below E_F. Increasing the overlayer thickness to 10 nm resulted in a 0.1 eV rigid shift of C_{60} levels towards lower BE. This shift was paralleled by the secondary

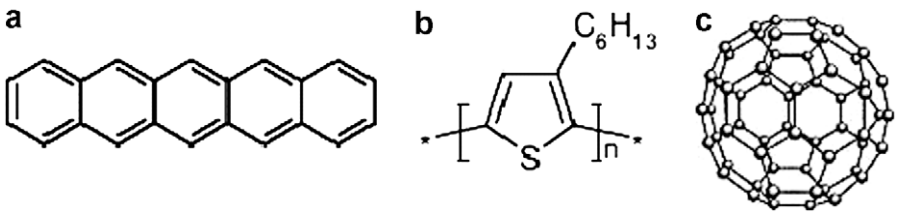

Fig. 1. Chemical structure of (a) pentacene, (b) P3HT, and (c) C_{60}.

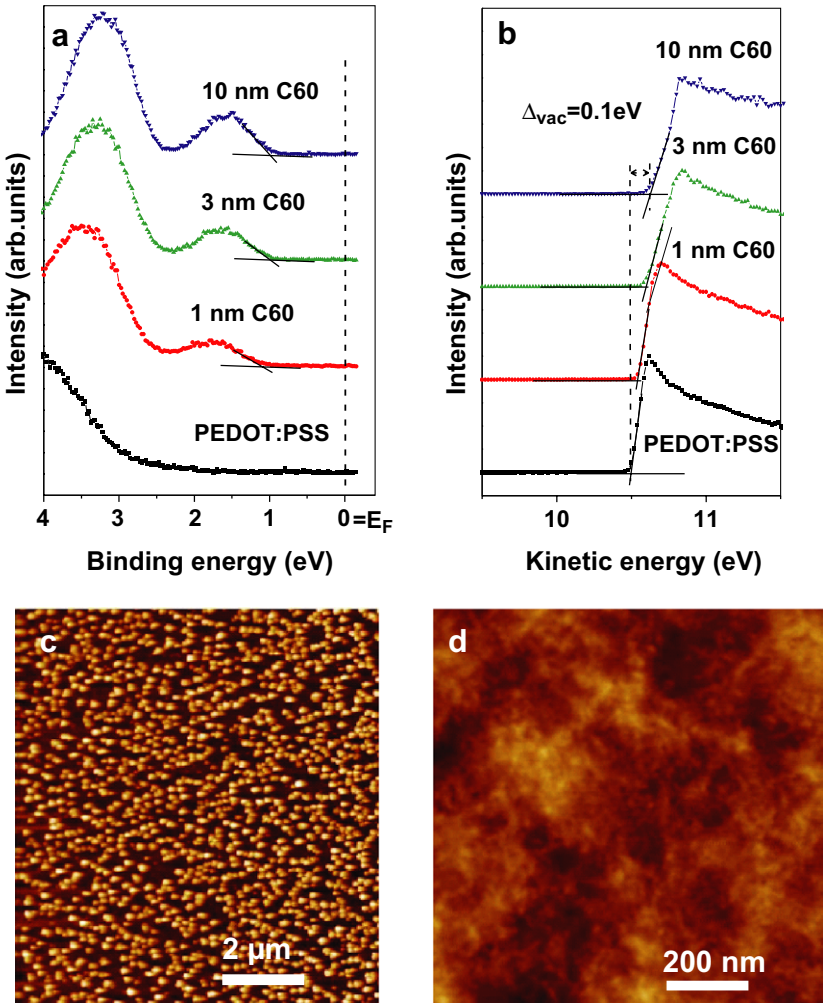

Fig. 2. (a) Valence region and (b) secondary electron cutoff photoemission spectra ($h\nu = 35$ eV) for increasing coverage of C_{60} on PEDOT:PSS/ITO. The intersections of the baselines with the tangents to the photoemission features are shown, indicating how the position of the low BE photoemission onset and the secondary electron cutoff was determined. AFM micrographs of (c) 10 nm C_{60} on PEDOT:PSS (120 nm height scale), and (d) PEDOT:PSS/ITO (10 nm height scale).

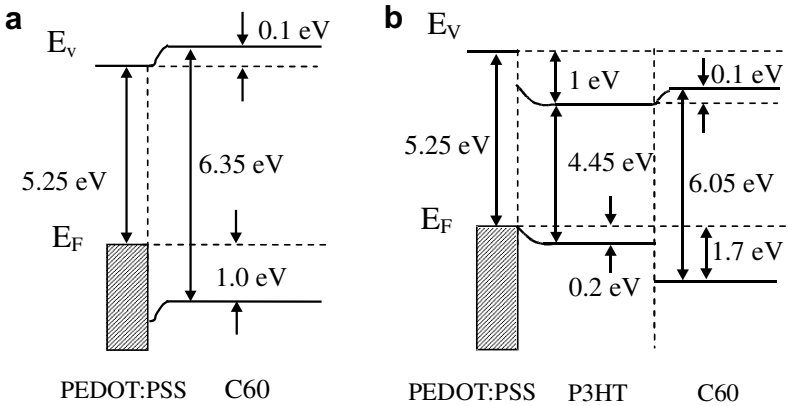

Fig. 3. Schematic energy level diagrams of the interfaces (a) C_{60}/PEDOT:PSS, and (b) C_{60}/P3HT/PEDOT:PSS. The vacuum level shift across the interface and the ionization energy of C_{60} must be regarded as lower limits, as uncovered PEDOT:PSS surface patches may yield too low work function values (see text).

electron cutoff, as shown in Fig. 2b. Thus, an interface dipole between C_{60} and PEDOT:PSS of +0.1 eV was formed, which is very close to the limit of vacuum level alignment. One might speculate that molecular level bending away from the direct interface to the conducting polymer was observed [6], since most of the 0.1 eV shift occurred between 3 nm and 10 nm of C_{60} nominal coverage. However, AFM images for 10 nm C_{60}/PEDOT:PSS (Fig. 2c and d) revealed that the film formed by C_{60} was not homogeneous, and rather small area islands with large heights were formed (pronounced island growth), compared to the rather smooth PEDOT:PSS surface. As a consequence, even at 10 nm nominal C_{60} thickness possibly bare PEDOT:PSS surface areas still existed, making a clear-cut statement on molecular level bending unattainable at this point. The ionization energy (IE) of C_{60} determined under these experimental conditions was 6.35 eV, which must be regarded as lower limit, as the secondary electron cutoff is an area-averaged measure of the sample work function. Conse-

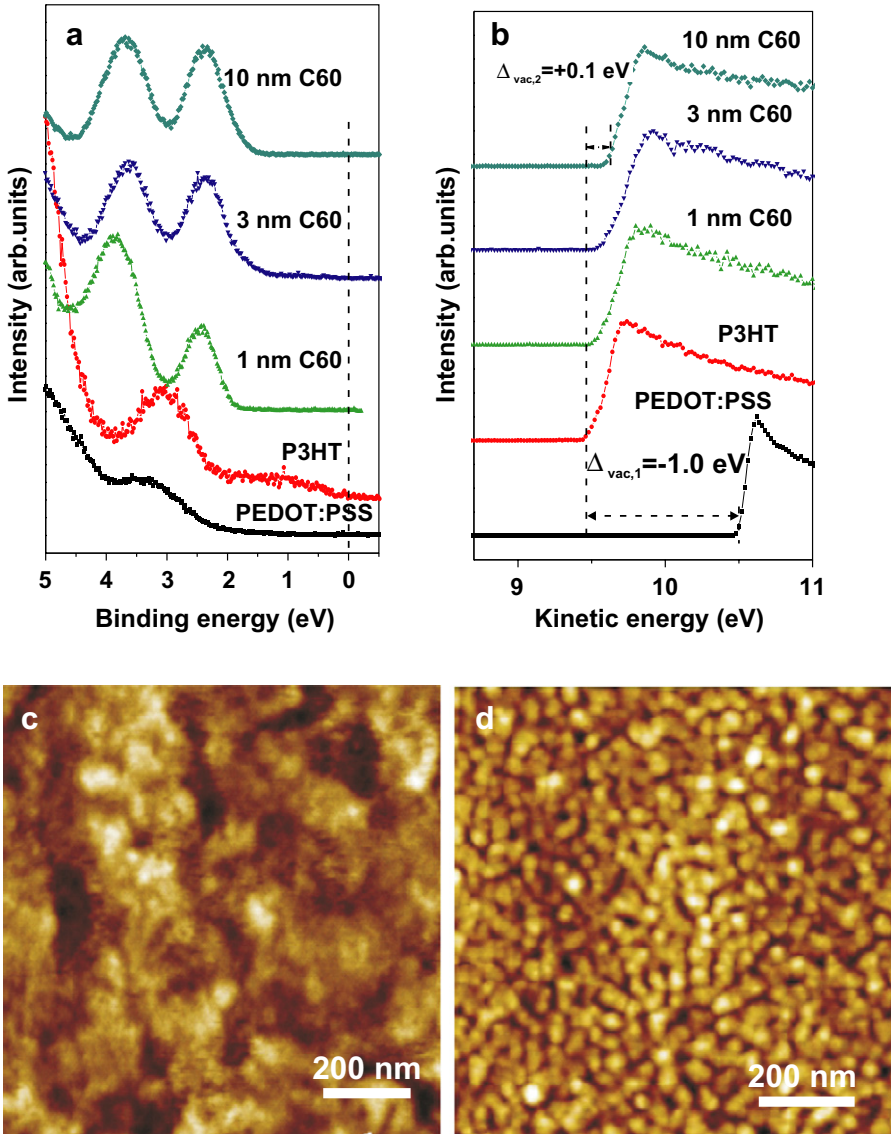

Fig. 4. (a) Valence region and (b) secondary electron cutoff photoemission spectra ($h\nu = 45$ eV) for increasing coverage of C_{60} on P3HT/PEDOT:PSS. AFM micrographs of (c) P3HT/PEDOT:PSS (10 nm height scale), and (d) 10 nm C_{60} on P3HT/PEDOT:PSS (25 nm height scale).

quently, contributions from still uncovered PEDOT:PSS (see above) lead to too low values for work function and ionization energy. A schematic diagram of the electronic structure for C_{60}/PEDOT:PSS summarizes these results (Fig. 3a). Note that only occupied levels are shown in all schematics, as unoccupied levels cannot be determined from UPS and consequently would posses a considerable error bar [15].

3.2. C_{60} on P3HT/PEDOT:PSS

Now we turn towards C_{60} deposited on P3HT pre-covered PEDOT:PSS. To start with, we discuss the P3HT/PEDOT:PSS interface. AFM showed that the P3HT morphology (Fig. 4c) closely resembled that of pristine PEDOT:PSS, and no detailed structures were observed on a nanoscopic scale. The appearance of crystalline grains for P3HT has been reported, however, on a flat Si-oxide substrate [17,18]. The hole injection barrier for P3HT was found to be only 0.2 eV from UPS (bottom-most curve in Fig. 4a), and a larger interface dipole of −1.0 eV was observed (Fig. 4b). This indicates that this interface is in the limiting case of Fermi-level pinning, due to the fact that P3HT polaronic levels determine the position of E_F within the energy gap of the polymer [19–21], leading to interfacial charge

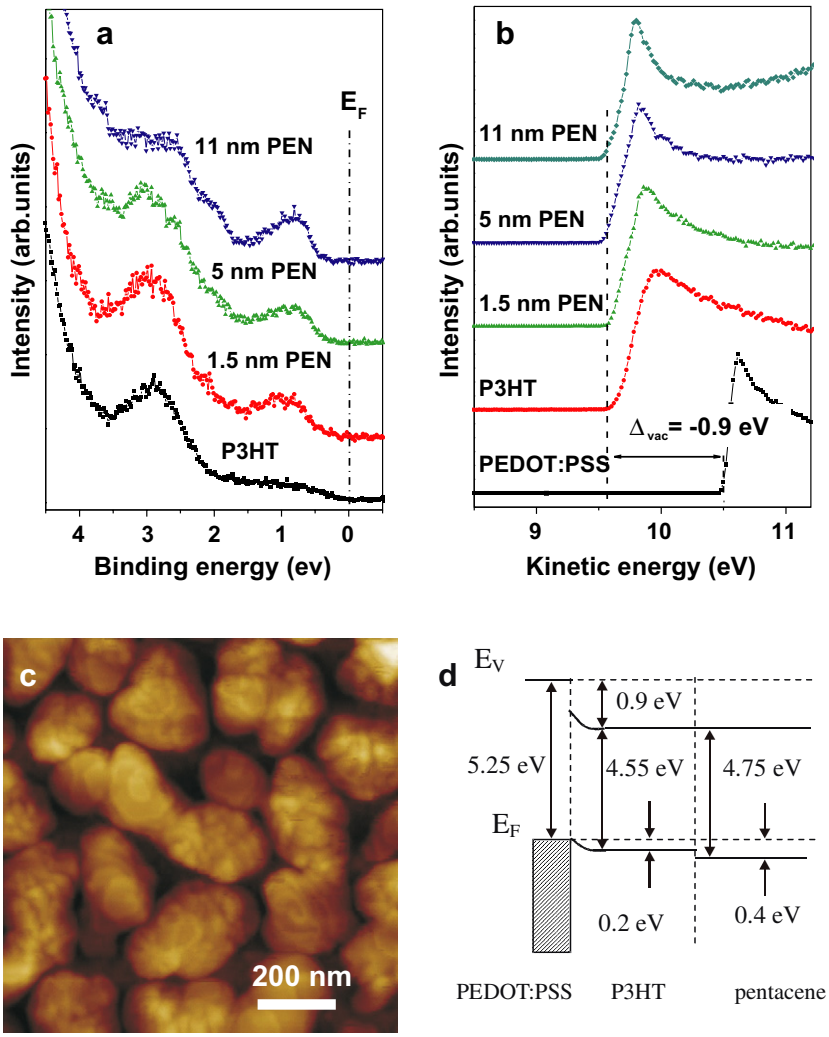

Fig. 5. (a) Valence region and (b) secondary electron cutoff photoemission spectra ($h\nu = 35$ eV) for increasing coverage of pentacene (PEN) on P3HT/PEDOT:PSS. (c) AFM micrograph of 11 nm pentacene on P3HT/PEDOT:PSS (30 nm height scale). (d) Schematic energy level diagram of the interface pentacene/P3HT/PEDOT:PSS.

transfer (positive charges on P3HT) that gives rise to the large interface dipole. Alternatively, due to the low ionization energy obtained for this P3HT film of *ca.* 4.45 eV, P3HT might undergo a similar charge exchange reaction at the PEDOT:PSS surface that was proposed for pentacene (ionization energy: *ca.* 5.0 eV) [22]. When depositing C_{60} onto P3HT/PEDOT:PSS, we observed the appearance of C_{60} photoemission features and an attenuation of P3HT signal, similar to C_{60} on PEDOT:PSS. However, the position of the energy levels was markedly different. The HOMO onset of C_{60} on P3HT/PEDOT:PSS was *ca.* 1.7 eV below E_F, and did not change as function of C_{60} thickness. The secondary electron cutoff position exhibited a shift of + 0.1 eV (= interface dipole) towards higher kinetic energy, *i.e.*, almost vacuum level alignment occurred at the C_{60}/P3HT interface. The ionization energy of C_{60} on P3HT/PEDOT:PSS was thus determined to be 6.05 eV, in agreement with literature [23]. This value is smaller than that of C_{60} on PEDOT:PSS, which could be due to the presence of still uncovered PEDOT:PSS surfaces patches (see Section 3.1). Note that the morphology of C_{60}/P3HT was markedly smoother than that for C_{60}/PEDOT:PSS (Fig. 4d).

The key result here is that the alignment of C_{60} energy levels relative to E_F was increased by 0.7 eV, by simply pre-coating PEDOT:PSS with a thin film of P3HT. This translates into PEDOT:PSS being a moderate hole injecting contact for C_{60}, while P3HT/PEDOT:PSS is a good electron injecting contact, which becomes strikingly evident when comparing the schematic energy level diagrams of the two different interfaces (Fig. 3a and b). Responsible for this is the charge transfer at the P3HT/PEDOT:PSS interface, which introduces a large interface dipole. C_{60} deposited onto P3HT/PEDOT:PSS aligns its levels relative to P3HT (essentially vacuum level alignment), but the effective substrate work function has already been decreased by the P3HT/PEDOT:PSS interface dipole of −1.0 eV.

3.3. Pentacene on P3HT/PEDOT:PSS

UPS spectra for increasing pentacene (PEN) coverage on P3HT/PEDOT:PSS are shown in Fig. 5a and b. In comparison to the P3HT/PEDOT:PSS shown in Fig. 2 the vacuum level shift was 0.1 eV smaller, which may indicate slight differences in the polymer film morphology; however, the valence band onset was not changed, and the overall reproducibility for other P3HT/PEDOT:PSS samples was better than 0.1 eV in our case. Most of the spectral features of P3HT disappeared already after 1.5 nm PEN coverage, and PEN features dominated for higher coverage. In particular, a clear peak evolves at *ca.* 0.9 eV BE, which is derived from the PEN HOMO. The low BE onset of the pentacene HOMO was 0.4 eV below E_F for all thicknesses, while the low BE onset of the P3HT valence band was 0.2 eV below E_F. No change in the position of the secondary electron cutoff was observed upon PEN deposition (Fig. 5b), indicating that vacuum level alignment prevails at the PEN/P3HT interface. The ionization energy of PEN was 4.75 eV. Such small values have been reported before for PEN films where the long molecular axes are oriented almost perpendicular to the substrate surface [15,24]. This type of molecular orientation was corroborated for the present sample by AFM (Fig. 5c), where individual step-heights corresponding to the length of a pentacene molecule (*ca.* 1.5 nm) were measured. Also, the PEN morphology on P3HT closely resembles that observed for PEN on PEDOT:PSS [22]. The schematic energy level diagram of PEN/P3HT/PEDOT:PSS interface is shown in Fig. 5d.

3.4. P3HT on pentacene/PEDOT:PSS

In order to investigate whether molecule-on-polymer and polymer-on-molecule interfaces exhibit the same energy level alignment, we first established that pentacene thin films are not significantly altered by treatment with the solvent used for P3HT. We

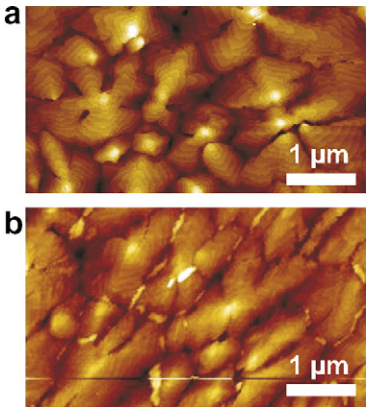

Fig. 6. AFM micrographs of 10 nm pentacene on native silicon oxide (a) before, and (b) after $CHCl_3$ treatment (40 nm height scale).

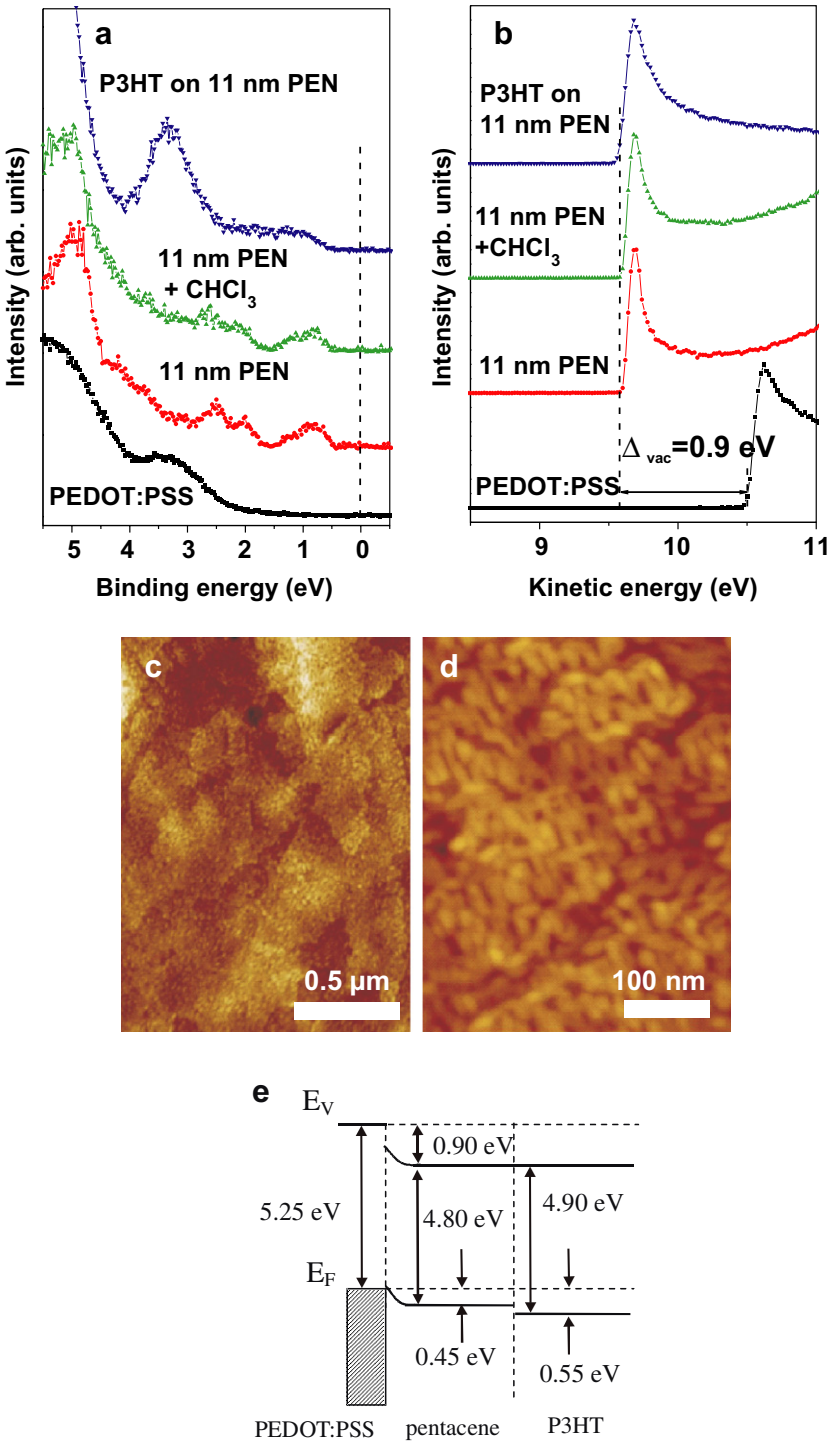

Fig. 7. (a) Valence region and (b) secondary electron cutoff photoemission spectra ($h\nu = 35$ eV) for 11 nm pentacene (PEN) on PEDOT:PSS before and after $CHCl_3$ treatment, and for P3HT spin-coated on top of pristine 11 nm PEN/PEDOT:PSS. (c) and (d) AFM micrographs of P3HT spin-coated onto 11 nm pentacene/PEDOT:PSS (15 nm height scale). (e) Schematic energy level diagram of the interface P3HT/pentacene/PEDOT:PSS.

simulated P3HT spin-coating onto PEN by employing identical spin-coating parameters (600 rpm) for chloroform alone. AFM showed that only minor changes of the PEN thin film morphology (for bet-

ter visibility with native silicon oxide as substrate) occurred, and the typical molecular step-heights were measured before and after $CHCl_3$ treatment (Fig. 6). Yet, some PEN probably was dissolved by $CHCl_3$ under our experimental conditions, as indicated by the fringed island edges. However, the solubility of PEN in $CHCl_3$ is very low, since even after soaking such PEN samples in copious amounts of $CHCl_3$ for 5 min removed only *ca.* 30% of the film mass (not shown).

Notably, also the electronic structure of the pentacene/PEDOT:PSS interface was not altered by $CHCl_3$ treatment (spin-coating of the solvent). The valance and secondary electron cutoff spectra for PEN on PEDOT:PSS before and after $CHCl_3$ treatment were virtually identical (Fig. 7a and b), and reproduced already published values for hole injection barrier (0.45 eV) and interface dipole (−0.9 eV) [22].

Consequently, spin-coating P3HT from $CHCl_3$ solution onto a PEN film should yield reliable photoemission results on the polymer-on-molecule electronic structure. In fact, UPS showed that vacuum level alignment at the P3HT/PEN interface prevailed (as was the case for PEN/P3HT), as no shift of the secondary electron cutoff occurred (Fig. 7b). However, the P3HT valence band onset was found 0.55 eV below E_F, *i.e.*, at 0.35 eV higher BE than for P3HT/PEDOT:PSS. At the same time, the ionization energy for the polymer-on-molecule case was 4.90 eV (compared to 4.45 eV and 4.55 eV for P3HT/PEDOT:PSS; see above). This change of ionization energy by ~0.4 eV is attributed to a different inter-molecular arrangement within P3HT on the molecular film substrate. This is supported by AFM images, which show that – in contrast to P3HT/PEDOT:PSS – small crystallite-like grains existed in the polymer overlayer (Fig. 7d). Larger scale images reveal that the P3HT film continuously covered the pentacene substrate, and the individual PEN steps could still be discerned (Fig. 7c). The energy levels at the P3HT/PEN/PEDOT:PSS interface are summarized in Fig. 7e.

4. Conclusions

The energy level alignment and morphology of interfaces formed between two molecular (C_{60}, PEN) and one polymeric (P3HT) organic semiconductors was investigated by UPS and AFM. As common substrate for all experiments the conducting polymer PEDOT:PSS was used. We found that the hole injection barrier for C_{60} was drastically larger on P3HT pre-coated PEDOT:PSS (1.7 eV) compared to pristine PEDOT:PSS (1.0 eV). This was facilitated by a large dipole (−1.0 eV) formed at the P3HT/PEDOT:PSS interface underneath the C_{60} layer. This effect of deposition-sequence-dependent energy level alignment needs to be considered when using multi-heterolayers in organic functional devices.

On the other hand, the hole injection barrier for pentacene was hardly affected by pre-coating PEDOT:PSS with P3HT (0.40 on P3HT/PEDOT:PSS *vs.* 0.45 eV on PEDOT:PSS). We attribute this to the fact that pentacene shows virtually the same interfacial dipole when deposited on PEDOT:PSS as does P3HT, and to a similar growth of PEN on both polymeric substrates. However, the valence band onset of P3HT was closer to E_F on PEDOT:PSS (0.2 eV) compared to PEN pre-covered PEDOT:PSS (0.55 eV). The ionization energy of P3HT on PEN/PEDOT:PSS was increased by almost the same amount. This was explained by different P3HT inter-molecular packing on the two substrates, which was corroborated by the observation by AFM of a disordered P3HT film on PEDOT:PSS and nanoscopic P3HT-related crystallites on PEN/PEDOT:PSS.

Acknowledgements

The authors thank H.C. Starck GmbH & Co. KG for providing PEDOT:PSS. This work was supported by the Sfb448 (DFG), the 863 project of the National High Technology Research and Development Program of China (No. 2006AA03Z0412), the 973 project of the National Grand Fundamental Research Program of China (No. 60576016), and the *Excellent Doctor's Science and Technology Innovation Foundation* of Beijing Jiaotong University (48011). NK acknowledges financial support by the Emmy Noether-Program (DFG).

References

[1] C.W. Tang, S.A. van Slyke, Appl. Phys. Lett. 51 (1987) 913.
[2] M. Pope, C.E. Swenberg, Electronic Processes in Organic Crystals and Polymers, Oxford University Press, Oxford, 1999.
[3] R.H. Friend, R.W. Gymer, A.B. Holmes, J.H. Burroughes, R.N. Marks, C. Taliani, D.D.C. Bradley, D.A. Dos Santos, J.L. Bredas, M. Löglund, W.R. Salaneck, Nature 397 (1999) 121.
[4] G. Hadziioannou, P.F. van Hutten (Eds.), Semiconducting Polymers, Wiley-VCH, Weinheim, 2000.

[5] B. Mazhari, Org. Electron. 6 (2005) 229.
[6] H. Ishii, K. Sugiyama, E. Ito, K. Seki, Adv. Mater. 11 (1999) 605.
[7] W.R. Salaneck, K. Seki, A. Kahn, J.-J. Pireaux (Eds.), Conjugated Polymer and Molecular Interfaces: Science and Technology for Photonic and Optoelectronic Applications, Marcel Dekker, New York, 2001.
[8] A. Kahn, N. Koch, W.Y. Gao, J. Polym. Sci. B 41 (2003) 2529.
[9] A. Rajagopal, C.I. Wu, A. Kahn, J. Appl. Phys. 83 (1998) 2649.
[10] S. Berleb, W. Brütting, G. Paasch, Synth. Met. 122 (2001) 37.
[11] W.Y. Gao, A. Kahn, Appl. Phys. Lett. 82 (2003) 4815.
[12] S.C. Veenstra, H.T. Jonkman, J. Polym. Sci. B 41 (2003) 2549.
[13] H. Vazquez, W. Gao, F. Flores, A. Kahn, Phys. Rev. B 71 (2005) 041306.
[14] O.V. Molodtsova, T. Schwieger, M. Knupfer, Appl. Surf. Sci. 252 (2005) 143.
[15] N. Koch, I. Salzmann, R.L. Johnson, J. Pflaum, R. Friedlein, J.P. Rabe, Org. Electron. 7 (2006) 537.
[16] A. Rajagopal, N. Koch, J. Ghijsen, K. Kaeriyama, R.L. Johnson, G. Leising, J.-J. Pireaux, Metallized Plastics 7 (2001) 1.
[17] S. Chao, K. Lee, J. Yuan, G.M. Wang, D. Moses, A.J. Heeger, J. Appl. Phys. 100 (2006) 114503.
[18] A. Zen, M. Saphiannikova, D. Neher, J. Grenzer, S. Grigorian, U. Pietsch, U. Asawapirom, S. Janietz, U. Scherf, I. Lieberwirth, G. Wegner, Macromolecules 39 (2006) 2162.
[19] C. Tengstedt, W. Osikowicz, W.R. Salaneck, I.D. Parker, C.H. Hsu, M. Fahlman, Appl. Phys. Lett. 88 (2006) 053502.
[20] S. Rentenberger, A. Vollmer, E. Zojer, R. Schennach, N. Koch, J. Appl. Phys. 100 (2006) 053701.
[21] N. Koch, A. Vollmer, Appl. Phys. Lett. 89 (2006) 162107.
[22] N. Koch, A. Elschner, J.P. Rabe, R.L. Johnson, Adv. Mater. 17 (2005) 330.
[23] S. Hasegawa, T. Miyamae, K. Yakushi, H. Inokuchi, K. Seki, N. Ueno, J. Electron Spectrosc. Relat. Phenom. 88–91 (1998) 891.
[24] H. Fukagawa, H. Yamane, T. Kataoka, S. Kera, M. Nakamura, K. Kudo, N. Ueno, Phys. Rev. B 73 (2006) 245310.